PROCEEDINGS OF SCIENCE

Formation of Copper Selenide synthesized by Mechanical Alloying

Vasileios Pavlidis,[a] Iordanis Karagiannis,[a] Nikolaos Sidiropoulos,[a] Aikaterini Teknetzi,[a] Lamprini Malletzidou,[a] Fani Stergioudi,[b] Nikolaos Michailidis,[b] George Vourlias[a] and Dimitrios Stathokostopoulos[a,*]

[a] *Laboratory of Advanced Materials & Devices, School of Physics, Faculty of Sciences, Aristotle University of Thessaloniki*
Thessaloniki, GR-54124, Greece

[b] *Physical Metallurgy Laboratory, Department of Mechanical Engineering, School of Engineering, Aristotle University of Thessaloniki*
Thessaloniki, GR-54124, Greece

E-mail: vaspavli@physics.auth.gr, iorkarag@physics.auth.gr, niksidir@physics.auth.gr, ateknetz@physics.auth.gr, labrinim@auth.gr, fstergio@meng.auth.gr, nmichail@meng.auth.gr, gvourlia@auth.gr, dstat@physics.auth.gr

Copper selenides are attractive materials for high-temperature thermoelectric applications. They exhibit remarkably enhanced thermoelectric properties originating from their superionic liquid character. In this work, the synthesis of Cu-Se compounds is investigated using mechanical alloying, aiming to obtain the Cu_2Se phase and modify the crystal structure by annealing at high temperatures and quenching. In the first part, Cu-Se powders are prepared at various milling times. They are characterized regarding their structure, morphology and composition by X-ray diffraction analysis and scanning electron microscopy. After 2.5 h of synthesis, α-Cu_2Se and β-Cu_2Se was attained in the powder, with the former having the highest percentage contribution. The crystallite size of these phases was calculated to be in the range of 17.0-19.6 nm. The synthesized powder consisted of grains with dimensions from nanometers to micrometers and their aggregates. A trace of a possibly surficial layer of copper oxide was also detected on the sample. In the second part of this study, the optimum synthesized powder was subjected to 2 h of annealing at 650 °C, followed by quenching. According to X-ray diffraction analysis, the percentage contribution of the thermoelectrically inferior α-Cu_2Se phase increased being the vast majority of the material and almost eliminated β-Cu_2Se. The crystallite size was calculated to be in the range of 31.2-34.5 nm. Overall, the desired Cu_2Se compound can be obtained by the mechanical alloying technique as α- and β-phase, and the crystal structure can be modified by annealing under appropriate conditions.

11th International Conference of the Balkan Physical Union (BPU11),
28 August - 1 September 2022
Belgrade, Serbia

[*] Speaker

PoS(BPU11)210

1. Introduction

Due to the emergence of energy and economic crisis and the concerns over climate change, there is an urgent need to develop sustainable technologies for better energy management. Thermoelectric (TE) technology can be the solution for industrial and everyday applications, as it exploits the recovered waste heat for power generation, being free of greenhouse emissions, noiseless and without mechanical parts requiring maintenance. The efficiency of TE materials can be determined by the dimensionless figure of merit (zT) [1] which is described as:

$$zT = \frac{S^2\sigma T}{\kappa_t} = \frac{S^2\sigma T}{\kappa_L + \kappa_e}$$

where S, σ, κ_t, T are the Seebeck coefficient, the electrical conductivity, the total thermal conductivity and the absolute temperature, respectively. The total thermal conductivity is the sum of two contributions, the electronic part (κ_e) and the lattice thermal conductivity (κ_L). Specifically, for medium to high temperature industrial applications (400 – 700 °C), Cu-Se alloys can achieve high zT due to superionic behavior above 100 °C [2]. This phase exhibits a superionic liquid behavior possessing enhanced TE properties. It is worth mentioning that these alloys, compared to other TE materials intended for the same temperature range such as $CoSb_3$ and PbTe, have the advantages of lower cost and environmental friendliness, since they do not contain the highly toxic elements of lead and cobalt [3], [4].

The binary system Cu-Se includes various phases at equilibrium, e.g. CuSe, Cu_2Se, non-stoichiometric $Cu_{2-x}Se$, Cu_3Se_2 and $CuSe_2$ [5]. In particular, Cu_2Se has two phases, α– and β–phase. The β-phase crystallizes in cubic structure, while three crystal structures have been reported for α-phase, i.e. tetragonal, orthorhombic and monoclinic. A transition from α– to β–phase takes place at 120 °C [6]. Due to the complexity of the binary phase diagram and the sublimation of Se at high temperatures, the synthesis of Cu_2Se or Cu_2Se-based materials is rather challenging. However, a variety of techniques, including solid-state reaction [7], spark plasma sintering [8], [9], mechanical alloying (high energy ball milling) [10], melting [11] and sputtering [12], have been used to synthesize these materials. β-Cu_2Se exhibits superior thermoelectric performance and through optimization a maximum zT value of about 2.7 has been achieved for this material [13].

In this work, a synthesis study of the Copper – Selenium material system is presented. The primary goal was to prepare Cu_2Se powder via Mechanical Alloying (MA) with variable milling time, in order to detect the optimal time that provides thermal stability and low risk of contamination. It is a solid-state powder technique with the following advantages: low cost, simplicity and eco-friendliness since no toxic fumes are released during the synthesis process. The main effect of this technique is to obtain finer powder and induce the formation of 0D, 1D and 2D defects, in order to intensify phonon scattering and, therefore, reduce lattice thermal conductivity. In addition, a selected synthesized sample was annealed, aiming to detect any changes in its crystal structure. The samples were thoroughly characterized regarding their structure, morphology and chemical composition.

2. Experimental Section

The different Cu_2Se samples were prepared following a specific standard procedure. Copper (purity 99.9%, < 45 μm) and Selenium (purity 99.5%, < 45 μm) powders -both been

supplied by Thermo Fisher Scientific- were weighed on a precision balance at 2:1 stoichiometric ratio. The mixture of the two powders was then introduced into the agate ball milling vessel containing twenty-five (25) agate balls of 10 mm diameter. The volume ratio of the balls to the inner side of the milling vessel was about 80%. The vessel was then sealed and inert gas (argon) was introduced through suitable valves to reduce the oxygen level to a minimum. Mechanical Alloying (MA) synthesis was carried out using a FRITSCH Planetary Micro Mill PULVERISETTE 7. MA was performed for three-time intervals of 1 h, 2 h and 2.5 h by the planetary ball milling process at rotational speeds of 500 rpm. Finally, annealing was carried out at 650 °C for 2 h under inert atmosphere, followed by quenching in salt-water (10 % w/w salt ratio). Before the annealing the sample was placed in a ceramic crucible and sealed to prevent oxidation.

A/A	*Experimental conditions*	*Sample Code Name*
1	Ball Milling – 1 h – 500 rpm	BM1
2	Ball Milling – 2 h – 500 rpm	BM2
3	Ball Milling – 2.5 h – 500 rpm	BM3
4	Ball Milling – 2.5 h – 500 rpm Annealed – 650 °C – 2 h – Quenched	BMA

Table 1: *Experimental conditions of the synthesized samples and given code names.*

The structural and phase identification was performed by X-ray diffraction (XRD) analysis using a 2-cycle Rigaku Ultima^{+} powder X-ray diffractometer with copper source (Cu Ka radiation), operating at 40 kV/30 mA. The morphology and the chemical composition of the powders were examined by scanning electron microscopy (SEM) measurements, carried out using a JEOL JMS-390LV microscope equipped with an OXFORD INCA 300 EDS analyser.

3. Results and Discussion

3.1 Study of the Mechanical Alloying Synthesis

In this section, samples BM1, BM2 and BM3 prepared at the milling times of 1 h, 2 h and 2.5 h, respectively, are discussed. Each sample was studied using XRD and a comparative graph of their patterns is presented in Fig. 1. In samples BM1 and BM2, some intense peaks at 2θ = 43.3°, 50.4° and 74.1° are observed indicating the existence of Cu (PDF #85-1326) [14]. Moreover, in these two samples, some intense peaks at 2θ = 23.5°, 29.7° and 43.6° are detected which indicate the presence of Se (PDF#73-0465) [14]. The relative intensity of Cu peaks is stronger in sample BM2 than in sample BM1, whereas the relative intensity of Se peaks is lower for BM2 than BM1. In addition, small peaks at 2θ = 28.1°, 31.1°, 46.0° and 49.9°, corresponding to a hexagonal crystal structure CuSe (PDF# 49-1457) [14], are detected in the pattern of sample BM1. On the contrary, in sample BM2, intense peaks at 2θ = 26.4°, 27.6°, 27.9°, 31.1° and 45.3° are spotted, identified as orthorhombic CuSe crystal structure (PDF#27-0184) [14]. Therefore, it is observed that CuSe appears with different crystal structure in BM1 and BM2. The peaks found in the pattern of sample BM2 at 2θ = 29.2°, 32.7°, 35.9° and 54.0° indicate the existence of a cubic $CuSe_2$ crystal structure (PDF#65-1846) [15, 16]. None of the above crystal structures are found in sample BM3. The intense peaks at 2θ = 13.0°, 26.2°, 26.4° and 43.9° indicate the existence of orthorhombic crystal structure Cu_2Se_x (PDF#47-1448). The intense peaks at 2θ = 13.1°, 26.3°, 43.9° and 51.8° are attributed to tetragonal crystal structure

Cu_2Se (PDF#29-0575) [14]. In addition, the peaks detected at 2θ = 26.6°, 44.2° and 52.4° can be ascribed to the cubic Cu_2Se crystal structure (PDF#88-2044). Finally, the peaks at 2θ = 26.8°, 44.4° and 52.6° are identified as cubic $Cu_{1.8}Se$ crystal structure (PDF#71-0044) [14]. At this point, it should be noted that label α–phase Cu_2Se in Fig.1 refers to both tetragonal Cu_2Se and orthorhombic Cu_2Se_x while label β–phase Cu_2Se refers to both cubic Cu_2Se and cubic $Cu_{1.8}Se$. It is observed that both α– and β–Cu_2Se phases are obtained during the synthesis time of 2.5 h. Lia et al. also reported in their study on Cu-Se system that single-phase β-Cu_2Se cannot be obtained during short synthesis time; it coexists with α-Cu_2Se and other Cu – Se phases [16].

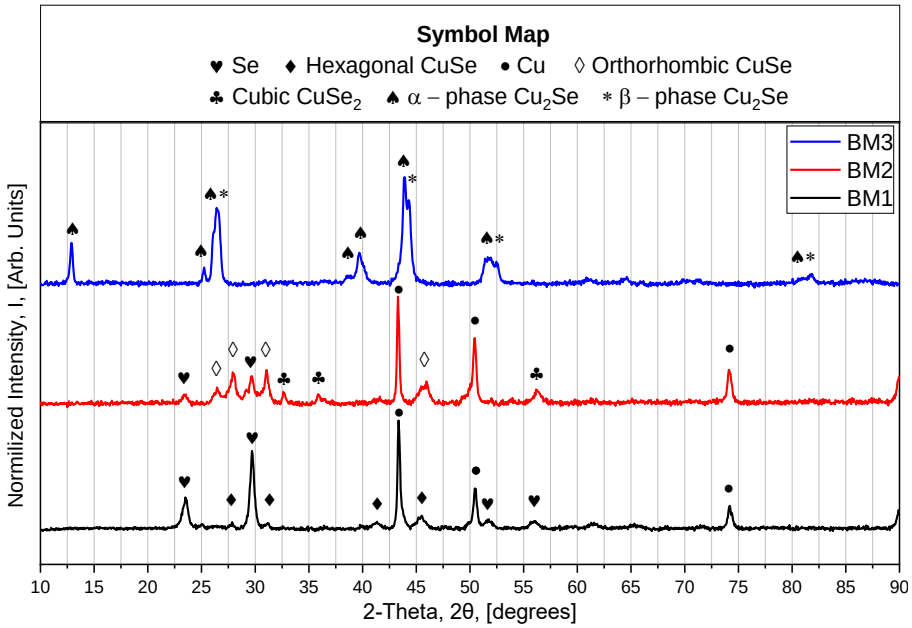

Figure 1: *Comparative graph of the XRD patterns of Cu - Se powders BM1, BM2 and BM3.*

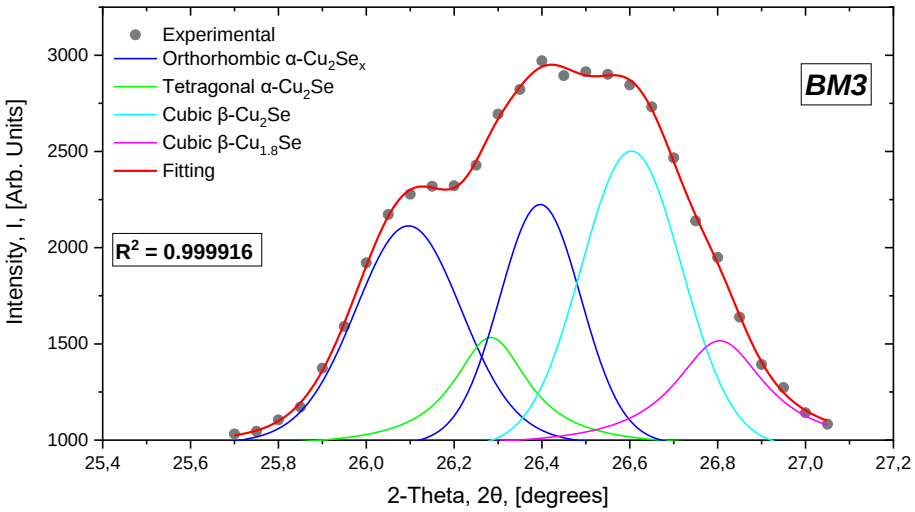

Figure 2: *Fitting simulation of the diffraction angle 2θ=27° of the XRD pattern of BM3.*

The fitting of the main peak at 27° confirmed the existence of all four different crystal structures (FullProf.2 k-Version 7.20 program [17]). Therefore, with these initial conditions, one manages to obtain Cu_2Se. Overall, it is clear that the samples differ strongly in terms of the crystal structures that they contain. Below are listed the main findings of the comparison of their

XRD patterns.

1. It is evident that the reaction between the pure elements proceeds as the milling time increases. The mechanism of copper selenide synthesis is a diffusion-controlled solid-state reaction. Hence, the longer the milling time, the more the pure elements (especially Cu) will diffuse. This results in the formation of phases close to the desired stoichiometry.
2. Regarding the relative intensity of Cu and Se peaks in samples BM1 and BM2, the following explanation can be given. $CuSe_2$ phase formed in sample BM2 requires twice as much Se as Cu. Therefore, a large amount of the unreacted Se found in BM1 has now been used for this new phase, leading to a decrease in the intensity of the corresponding peaks.
3. As MA time increases (in the interval from 1 h to 2.5 h), the amount of unreacted pure elements Cu and Se decreases until they are depleted in the case of 2.5 h ball milling.

More specifically, sample BM3 exhibits a strong peak at 13°, which is not detected in the other two samples. This implies the existence of α-phase Cu_2Se in the former and its absence in the other two. Furthermore, a strong peak is detected at 26.5° in the pattern of BM3. In the other two cases a strong peak is detected at 23.5°. This highlights the presence of α-phase Cu_2Se in the former and pure Se in the other two samples. At the region of 44°, BM3 shows strong peaks at 44° and 44.5° while in the other two cases strong peaks are identified at 43.5° and 50.5°. The presence of α-phase Cu_2Se and β-phase Cu_2Se in the former and pure Cu in the other two samples is indicated.

The above results can be explained according to Fick's first law [18]. It states that the diffusion flux is proportional to the diffusion coefficient and the concentration gradient. Therefore, the amount of material transferred from one region of matter to another by diffusion depends on a number of factors, mainly time. The degree of reaction increases with the extension of the Ball Milling time because the mass transfer is proportional to time. Thus, by increasing the milling time, the pure elements -especially Cu -diffuse in space creating new crystal structures [16].

3.1.1 Analysis of Crystallographic Constants and Characteristics of the Produced Structures

At this point of the study, it is necessary to calculate the crystallographic constants of the three samples. The experimental values are compared with the theoretical ones retrieved from the PDF used for indexing [14]. The calculation of the experimental values of the crystallographic constants was performed by applying Bragg's law [19] and the results of this study are presented in Table 2. The percentage error of the calculated values was 0.02%-0.14%.

The area of each diffraction peak was studied and their full width at half maximum (FWHM) was calculated (FullProf.2 k-Version 7.20 program [17]), aiming to determine the percentage contribution of each crystal structure to the synthesized powder as well as the crystallite size. The crystallite size was calculated by the Debye-Scherrer formula ($d = 0.9 \cdot k/\beta \cdot \cos(\theta)$), where k is the wavelength of the X-ray, b is the full width at half maximum and θ is the Bragg's angle of reflection. Bar graphs with the summarized results are presented in Fig. 3. In Fig. 3(a), the crystallite sizes of the different crystal structures are demonstrated. It is widely known that, as the milling time increases, the crystallite size of each phase decreases [20]. However, in this work, no identical phases are found between the samples so such a

comparison cannot be made. In all three cases, BM1, BM2 and BM3, the size of the crystallites of the crystal structures is within the range of 12.0-22.0 nm. The size of the crystallites is verified by previous studies indicating that with this synthesis technique, the crystal structures are in the nano-dimensions [20, 21].

BM1		**BM2**		**BM3**	
Compound	*Exp. Value*	*Compound*	*Exp. Value*	*Compound*	*Exp. Value*
Se	a = 4.360 Å c = 4.952 Å	Se	a = 4.368 Å c = 4.950 Å	Cu_2Se (Tet.)	a = 11.515 Å c = 11.753 Å
CuSe	a = 14.215 Å c = 17.238 Å	CuSe	a = 3.946 Å b = 6.964 Å c = 17.225 Å	Cu_2Se_x	a = 13.803 Å b = 20.382 Å c = 3.928 Å
Cu	a = 3.612 Å	Cu	a = 3.611 Å	Cu_2Se (Cub.)	a = 5.793 Å
-	-	$CuSe_2$	a = 6.122 Å	$Cu_{1.8}Se$	a = 5.770 Å

Abbreviations: Exp. Value → Experimental Value, Tet. → Tetragonal, Cub. → Cubic

Table 2: *Lattice parameters calculated for the Cu – Se powders BM1, BM2 and BM3 synthesized under different experimental conditions.*

In Fig. 3(b), the percentage contribution of each crystal structure to the produced samples is presented. It is observed that, after 1 h of MA at a rotational speed of 500 rpm (BM1), pure Cu predominates in the structure followed by Se and CuSe. After a 2-h MA process (BM2), CuSe predominates followed by pure Cu, pure Se and $CuSe_2$. Finally, after 2.5 h of MA, α-Cu_2Se predominates with a total percentage of 65% followed by β-Cu_2Se with a total percentage of 35 %. These ratios verify the results of previous studies at which the importance of longer milling time for achieving the desired 2:1 stoichiometry was emphasized [16].

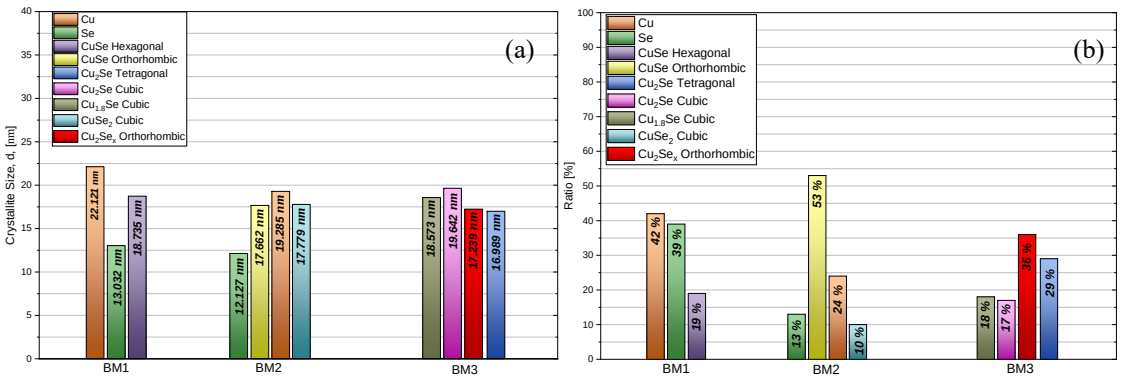

Figure 3: *Bar graph of (a) the size of the crystallites, and (b) the percentage contribution of each crystal structure to the Cu - Se samples BM1, BM2 and BM3 synthesized at different experimental conditions.*

3.1.2 Morphological Characterization of Selected Sample

According to the information collected so far by XRD analysis, the desired crystal structure in stoichiometry 2:1 is formed in sample BM3, which is synthesized by a 2.5 h MA process. At this part of the study, the investigation of the sample using SEM analysis is presented. The morphology and chemical composition of the as-prepared copper selenide powder are examined.

Figure 4 shows representative SEM images of BM3 at different resolutions. The grains of the powder exhibit a "deformed sphere-like" morphology. The sample contains both large grains, ranging from 20 μm to 40 μm in size, and smaller grains of about 1-4 μm in size. In fact, the larger grains are agglomerations of the smaller ones, as the inset of Fig. 4(a) clearly shows.

Small grains, which have not come into close proximity to each other during synthesis to become compact, cover the surface of the agglomerations. Unwanted impurities may be entrapped in the gaps formed between them (yellow marking in Fig. 4(a)).

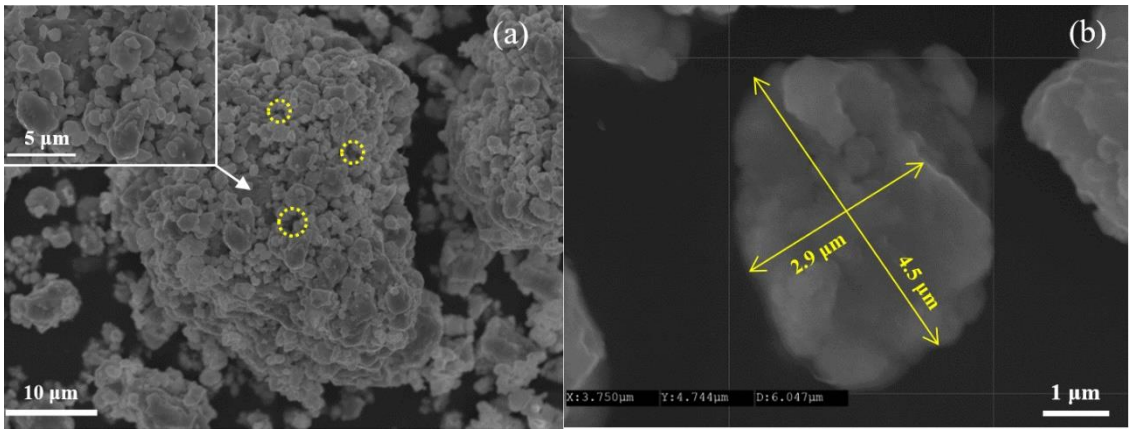

Figure 4: *SEM images of sample BM3 with magnification (a) x2,000 and (b) x12,000. The inset depicts a magnified region of the surface of the large grain (x8,000).*

In Fig. 4(b), a single small grain of the sample is shown. The dimensions of the grain are below 5 μm with a mean diameter of about 3.8 μm. It appears that this grain was probably formed by even smaller grains, approaching the nano-dimensions in size, which were in close contact during synthesis and became compact [22, 23]. Their dimensions may be between 200 nm and 700 nm. Therefore, it is concluded that the powder contains large grains (>20 μm) formed by the aggregation of smaller ones (>1 μm), with the latter being compactly composed of even smaller-sized grains (>200 nm). These observations are in good agreement with the study of Li et al. that reported on Cu-Se powders. The morphology of $Cu_{2-x}Se$ powder appears to be similar to that presented in the current study [24].

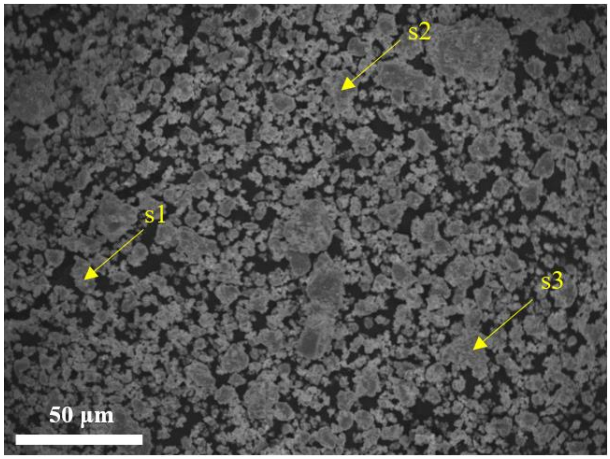

Figure 5: *Representative SEM image of sample BM3.*

Element	s1	s2	s3
Cu (at%)	67.55	62.86	63.42
Se (at%)	32.45	37.14	36.58

Table 3: *Indicative EDS analyses of sample BM3.*

EDS point measurements were performed in order to examine the elemental composition of the sample. Indicative analyses are shown in Fig.5 with code names s1, s2 and s3, and the results can be found in Table 3. The concentration of Cu ranges from 62.86 at% to 67.55 at%, while Se concentration is from 32.45 at% to 37.14 at%. The calculated Cu and Se concentrations are consistent with Cu_2Se and non-stoichiometric $Cu_{2-x}Se$ phases acquired by XRD analysis.

3.2 Modification of Crystal Structure by Annealing

As already mentioned, the 2:1 stoichiometry in the Cu-Se system is composed of two phases, the low temperature α-phase and the high temperature β-phase [7]. New crystal structures can be obtained above the transition temperature of 120 °C employing various techniques. Typically, annealing, in addition to improving the crystallinity of a material, [25] can be used to obtain different regions of the phase diagram. In particular, β-phase Cu_2Se can be attained by using rapid cooling after annealing under appropriate conditions [26]. Previous studies have identified the use of annealing in pure or doped Cu-Se system to provide the Cu_2Se cubic crystal structure i.e. the β-phase of Cu_2Se [27, 28, 29].

In this part of the study, an attempt to modify the synthesized BM3 sample by annealing is made. The sample was annealed at the temperature of 650 °C for 2 h and was subsequently quenched in salt-water.

After annealing, sample BMA in powder form was studied using XRD and its pattern is given in Fig. 6 along with that of sample BM3 for comparison. Label α–phase Cu_2Se refers to tetragonal Cu_2Se and orthorhombic Cu_2Se_x, while label β–phase Cu_2Se refers to cubic Cu_2Se and cubic $Cu_{1.8}Se$. In the pattern of sample BMA, intense peaks observed at 2θ = 13.0°, 26.2°, 26.4° and 43.9° indicate the existence of orthorhombic crystal structure Cu_2Se_x (PDF#47-1448) [14]. Furthermore, the peaks at 2θ = 26.8°, 44.4° and 52.6° correspond to the cubic $Cu_{1.8}Se$ crystal structure (PDF#71-0044) [14].

It is apparent from this study that sample BMA can be identified by only two crystal structures, in contrast to BM3 that requires four crystal structures. Consequently, the high temperature and the rapid cooling reinforce the existence of the orthorhombic crystal structure Cu_2Se_x and cubic crystal structure $Cu_{1.8}Se$ at the expense of the tetragonal crystal structure Cu_2Se and cubic crystal structure Cu_2Se. Moreover, it is noticed that the crystal structures obtained from this investigation are non-stoichiometric i.e. they do not fulfill the requirement of the Cu:Se ratio being 2:1. This is interpreted by the fact that Se sublimates at the temperature of 221 °C [30]. Therefore, at the high temperature that the annealing was carried out, part of Se sublimates, resulting in a lack of it in the final crystal structures. In any case, the applied annealing conditions, lead to the formation of the orthorhombic crystal structure Cu_2Se_x and the cubic crystal structure $Cu_{1.8}Se$. This result is in agreement with a previous study by R. Subas et al., at which no substantial improvement of the crystal structure was found at such high temperatures [26]. It is important to investigate lower annealing temperatures, around 300 °C, in order to achieve a higher contribution of β-phase Cu_2Se to the final material.

Comparing samples BM3 and BMA, they differ greatly regarding the crystal structures they contain. Some of the main observations are given below:

1. It is clearly observed that the annealing process at such high temperature has made the

peaks of the different crystal structures in the XRD pattern more distinct [25]. It is easy to distinguish the peaks belonging to the α-phase Cu_2Se and β-phase Cu_2Se. Concerning α-phase Cu_2Se in sample BMA, a single crystal structure is detected, i.e. orthorhombic Cu_2Se_x. Similarly, β-phase Cu_2Se includes only cubic $Cu_{1.8}Se$ in sample BMA.

2. The relative intensity of the α-phase Cu_2Se in the case of annealing is evidently much higher than the relative intensity of the β-phase Cu_2Se. This can practically mean that the annealing process favors the crystallization in the α-phase Cu_2Se.
3. Comparing these two XRD patterns, it is found that the peaks of the annealed sample are sharper than before annealing. Typically observed peaks are located in the region of 13°, 27° and 44°. According to Debye-Scherrer formula, the full width at half maximum (FWHM) of each peak and the size of the crystallite are inversely proportional. Therefore, it is identified that in the case of the annealed sample, BMA, the size of the crystallites increases.

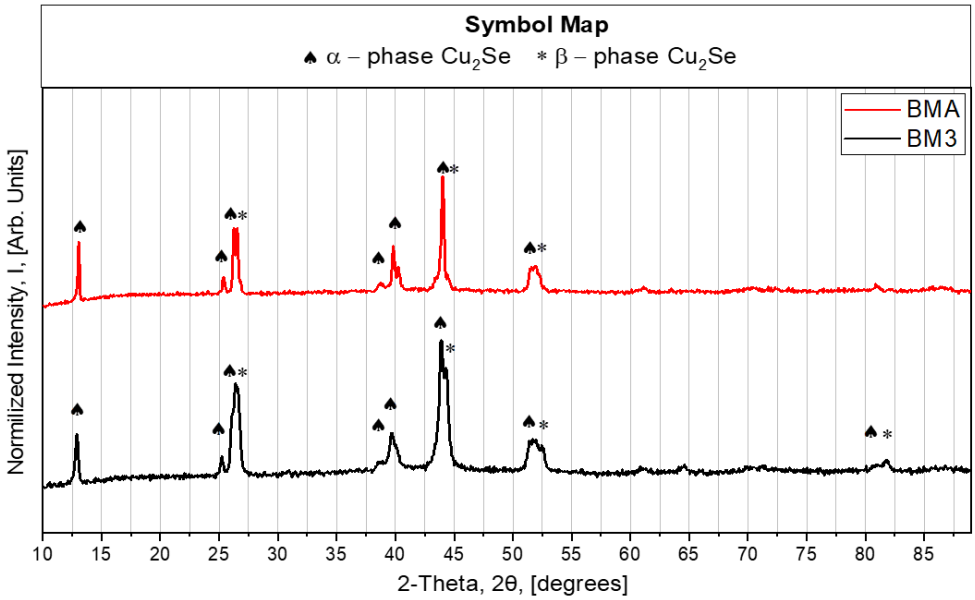

Figure 6: *Comparative graph of the XRD patterns of the Cu - Se samples BM3 and BMA.*

In the case of the annealed sample, the peak at 13° is slightly shifted towards higher angles compared to that without annealing. In addition, a decrease in the width of the peak of BMA as well as an increase in the relative intensity compared to sample BM3 is detected. At 27°, a relative shift of the diffraction peaks of BMA compared to BM3 is observed. Furthermore, in sample BMA, the separation of the peaks of the different crystal structures is clearly shown. On the contrary, an overall peak appears for all crystal structures in the pattern of sample BM3. Finally, the observations for 44° are similar to those already made for the two previous regions. A slight shift of the peaks and a clear separation of them for each crystal structure characterize the XRD patterns of sample BMA compared to sample BM3.

Overall, the crystal structure of sample BM3 is indeed modified using annealing. However, in order to obtain only the cubic β-phase Cu_2Se, the annealing conditions (annealing time and temperature) need to be further investigated.

3.2.1 Analysis of Crystallographic Constants and Characteristics of the Annealed Sample

The crystallographic constants of the annealed sample were experimentally calculated and then they were compared with the corresponding theoretical values. The results of these calculations are presented in Table 4.

BMA		
Compound	*Experimental Value*	*% Error*
Cu_2Se_x	a = 13.800 Å	0.05
	b = 20.378 Å	0.07
	c = 3.924 Å	0.02
$Cu_{1.8}Se$	a = 5.766 Å	0.02

Table 4: *Lattice parameters calculated for the Cu – Se powder BMA synthesized by MA process (2.5 h, 500 rpm), annealed at 650 °C for 2 h and quenched in salt-water.*

Comparing Tables 2 and 4, it is found that the experimental crystallographic constants of sample BM3 are slightly larger than those of sample BMA. This is expected since the diffraction peaks of the latter are shifted to higher angles, as already discussed in the previous section. The calculation of the experimental values of the crystallographic constants was done using the Bragg equation, as previously described for BM1, BM2 and BM3 [19].

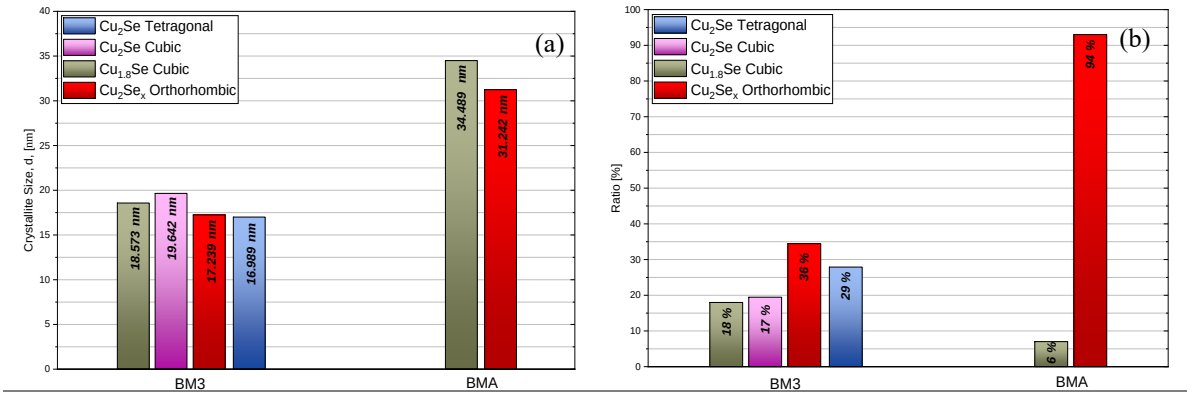

Figure 7: *Bar graph of* ***(a)*** *the size of the crystallites and* ***(b)*** *the percentage contribution of each crystal structure to the Cu - Se sample BMA synthesized by MA process (2.5 h, 500 rpm), annealed at 650 °C for 2 h and quenched in salt-water.*

The area of each diffraction peak was studied and their full width at half maximum (FWHM) was calculated (FullProf.2 k-Version 7.20 program). The crystallite size was calculated by applying the Debye-Scherrer formula, as already mentioned in Section 1.1.1. The bar graphs in Fig. 7 summarize the results of this analysis. Figure 7(a) presents the crystallite size of the different crystal structures, while Fig. 7(b) shows the percentage contributions of the different crystal structures to the synthesized samples. Regarding the crystallite size, variations between as-synthesized and annealed samples are found. After annealing, the crystallite size of both α-phase Cu_2Se and β-phase Cu_2Se increases. The former is increased by 14.0 nm, approximately, while the latter is increased by ~ 16.0 nm. These results confirm the observation in the XRD pattern, at which the width of the diffraction peaks was significantly reduced.

One main reason for this effect is that an increase in temperature leads to an increase in the crystallinity of the sample. More specifically, the annealing temperature provides the appropriate thermal energy to the system and atoms to migrate in the crystal structure,

eliminating the dislocations and structural defects. It is noted that these structural defects before annealing act as barriers preventing the enlargement of the crystallites, as they are located at their boundaries. Thus, crystallites can now increase their size without any restriction [31]. In addition, atoms that have received appropriate energy from annealing move within the crystal structure. These atoms interact with each other, creating new bonds and forming new structures. The outcome is the formation of new crystallites with considerably larger dimensions than those obtained under the initial conditions. These explanations agree with R. Napitupulu who studied the behavior of metals as a function of annealing temperature [32]. The behavior of the sample studied in this work has also been reported in a previous study by C. S. Sunandana et al. who studied thin films of copper selenide [31].

In Fig. 7(b), it is observed that the contribution of the α-phase Cu_2Se to sample BMA is much higher than that of the β-phase Cu_2Se. In particular, the percentage contribution of the α-phase Cu_2Se increases from 35% to 94%. Hence, a phase transition from the β - phase to the α-phase takes place under the applied annealing conditions. Further studies, using different annealing temperatures, need to be carried out to in order to gain a complete understanding of the phase transition of this crystal structure.

4. Conclusions

In this work, Cu-Se powders synthesized by the Mechanical Alloying (MA) technique were studied. The samples were prepared under different milling times from 1 h to 2.5 h. Unreacted Cu and Se, as well as CuSe, were identified by XRD analysis in the powders synthesized at short milling times up to 2 h. On the contrary, Cu_2Se was formed as two different phases, α-phase and β-phase, during 2.5 h of milling. The crystallite sizes of the different structures existing in the samples were calculated to be in the range of 12.0-22.0 nm, implying that the formed structures belong to the nano-dimensions. The percentage contribution of each structure to the powders was also determined. It was observed that, as the milling time increases, the contribution of pure elements Cu and Se decreases until they are depleted. α-phase Cu_2Se has the main contribution in the powder of 2.5 h. This sample was further examined by SEM analysis. The powder consists of grains of different sizes from nanoscale to microscale for the smaller grains form agglomerations. EDS measurements confirmed the presence of both Cu_2Se and $Cu_{2-x}Se$. Finally, an attempt was made to modify the crystal structure of the powder prepared in 2.5 h by annealing at 650 °C. The crystallite size increased after annealing by 14.0 nm for α-phase Cu_2Se and by 16.0 nm for β-phase Cu_2Se. α-phase Cu_2Se was calculated to be the vast majority of the annealed powder and the percentage contribution of the β-phase Cu_2Se was almost non-existent. Further investigation of the annealing conditions is needed. Overall, the Cu-Se powder prepared by Mechanical Alloying contains α-phase Cu_2Se and β-phase Cu_2Se. The crystal structure of Cu_2Se can be modified by annealing but appropriate conditions of temperature and time are required in order to obtain only cubic β-phase Cu_2Se.

Acknowledgments

This research was carried out as part of the project «Design and implementation of innovative lift's air-conditioning systems by using thermoelectric devices» (Project code: KMP6-0074109) under the framework of the Action «Investment Plans of Innovation» of the Operational

Program «Central Macedonia 2014 2020», that is co-funded by the European Regional Development Fund and Greece.

References

[1] D.M. Rowe, CRC Handbook of Thermoelectrics, CRC Press, USA, 1995.

[2] Chong Rae Park, Advanced Thermoelectric Materials, John Wiley & Sons, Ltd 2019.

[3] S. Kumar, M. K. Gupta, P. Goel, R. Mittal, O. Delaire, A. Thamizhavel, S. Rols, S. L. Chaplot, *Solid-like to Liquid-like Behavior of Cu Diffusion in Superionic Cu_2X (X=S, Se): An Inelastic Neutron Scattering and Ab-Initio Molecular Dynamics Investigation*, *Phys. Rev. Materials* (2022) [doi.org/10.48550/arxiv.2201.00606].

[4] L. Xue, C. Fang, W. Shen, M. Shen, W. Ji, Y. Zhang, Z. Zhang, X. Jia, *Thermoelectric properties of S-doped Cu2Se materials synthesized by high-pressure and high-temperature method*, *Mod Phys Lett B* (2019) [doi.org/10.1142/S0217984920500062].

[5] D.J. Chakrabarti, D.E. Laughlin, *The Cu−Se (Copper-Selenium) system*, *Bulletin of Alloy Phase Diagrams 2*, 305–315 (1981), [doi.org/10.1007/BF02868284].

[6] B. Koren, O. Friedman, N. Maman, S. Hayun, V. Ezersky, Y. Golan, *Sample preparation induced phase transitions in solution deposited copper selenide thin films*, *RSC Adv.* **12** (2022) 277 [doi.org/10.1039/D1RA07947F].

[7] N. Roth, B. B. Iversen, *Solving the disordered structure of β-Cu2−xSe using the three-dimensional difference pair distribution function*, *Advanced Materials* **32** (2019) [doi.org/10.1107/S2053273319004820].

[8] K. Zhao, H. Duan, N. Raghavendra, P. Qiu, Y. Zeng, W. Zhang, J. Yang, X. Shi, L. Chen, *Solid-State Explosive Reaction for Nanoporous Bulk Thermoelectric Materials*, *Advanced Materials* **29** (2017) [doi.org/10.1002/ADMA.201701148].

[9] P. Nieroda, A. Kusior, J. Leszczyński, P. Rutkowski, A. Koleżyński, *Thermoelectric Properties of Cu2Se Synthesized by Hydrothermal Method and Densified by SPS Technique*, *Materials* **14** (2021) [doi.org/10.3390/MA14133650].

[10] S. Butt, M. U. Farooq, W. Mahmood, S. Salam, M. Sultan, M. A. Basit, J. Ma, Y. Lin, C.W. Nan, *One-step rapid synthesis of Cu2Se with enhanced thermoelectric properties*, *J Alloys Compounds* (2019) [doi.org/10.1016/J.JALLCOM.2019.01.359].

[11] J. Liu, M. Li, S. Yang, S. Zhang, J. Feng, C. Li, P. Zhang, L. Zhou, *Enhanced thermoelectric and mechanical properties in hierarchical tubular porous cuprous selenide*, *Scripta Materialia* (2020) [doi.org/10.1016/J.SCRIPTAMAT.2019.09.009].

[12] P. Fan, X.-l. Huang, T. Chen, F. Li, Y. Chen, B. Jabar, S. Chen, H. Ma, G. Liang, J. Luo, X. Zhang, Z. Zheng, *α-Cu2Se thermoelectric thin films prepared by copper sputtering into selenium precursor layers*, *Chemical Engineering Journal* (2021) [doi.org/10.1016/J.CEJ.2021.128444].

[13] Z. Zhang, K. Zhao, T. R. Wei, P. Qiu, L. Chen, X. Shi, *Cu2Se-Based liquid-like thermoelectric materials: looking back and stepping forward*, *Energy Environ Sci*. (2020) [doi.org/10.1039/D0EE02072A].

[14] International Centre for Diffraction Data (ICDD) (Formerly Joint Committee on Powder Diffraction Standards- JCPDS), *Powder Diffraction File (PDF)*, 2003.

[15] A. Stevels, F. Jellinek, *Phase transitions in copper chalcogenides: Copper-selenium system, Recl. Trav. Chim. Pays-Bas* **90** (1971) 273 [doi.org/10.1002/recl.19710900307].

[16] J. Lia, G. Liu, X. Wua, G. He, Z. Yang, J. Li, *Reaction mechanism in mechanochemical synthesis of $Cu_{2-x}Se$, Ceram. Int.* **44** (2018) 22172 [doi.org/10.1016/j.ceramint.2018.08.331].

[17] J. Rodríguez-Carvajal, *Recent advances in magnetic-structure determination by neutron powder diffraction, Phys. B*, 192 (1993) 55–69 [doi.org/10.1016/0921-4526(93)90108-I].

[18] L. Wang, *A general theory of diffusion, Prog. Theor. Phys.* **101** (1999), 541 [doi.org/10.1143/PTP.101.541].

[19] H.W. Bragg, L.W. Bragg, *The reflection of X-rays by crystals, Proc. R. Soc. A.* **88** (1913) 428 [rspa.1913.0040].

[20] Rajkovic, E. Romhanji, M. Mitkov, *Characterization of high-energy ball milled prealloyed copper powdercontaining 2.5 wt%Al*, *J. Mater. Sci. Lett.* **21** (2002) 169 [doi.org/10.1023/A:1014209618494].

[21] A. Muthukannan, G. Sivakumar, K. Mohanraj, *Influence of Equimolar Concentration on Structural and Optical Properties of Binary Selenides Nanoparticles, Part. Sci. Technol.* **32** (2014) 392 [doi.org/10.1080/02726351.2014.880978].

[22] D. Li, X. Y. Qin, Y. F. Liu, C. J. Song, L. Wang, J. Zhang, H. X. Xin, G. L. Guo, T. H. Zou, G. L. Sun, B. J. Ren, X. G. Zhu, *Chemical synthesis of nanostructured Cu_2Se with high thermoelectric performance, RSC Adv.* **4** (2014) 8638 [doi.org/10.1039/C3RA47015F].

[23] L. Xue, Z. Zhang, W. Shen, H. Ma, Y. Zhang, C. Fang, X. Ji, *Thermoelectric performance of Cu_2Se bulk materials by high-temperature and high-pressure synthesis, J. Materiomics* **5** (2018) [doi.org/10.1016/j.jmat.2018.12.002].

[24] L. Li, Y. Zhao, C. Shi, W. Zeng, B. Liao, M. Zhang, X. Tao, *Facile synthesis of copper selenides with different stoichiometric compositions and their thermoelectric performance at a low temperature range, RSC Adv* **11** (2021) 25955 [doi.org/10.1039/D1RA04626H].

[25] J. D. Forster, J. J. Lynch, N. E. Coates, J. Liu, H. Jang, E. Zaia, M. P. Gordon, M. Szybowski, A. Sahu, D. G. Cahill, J. J. Urban, Solution-Processed Cu_2Se Nanocrystal Films with Bulk-Like Thermoelectric Performance, Scientific Reports **7** (2017) [doi.org/10.1038/s41598-017-02944-1].

[26] R. Subas, G. Statkute, I. Mikulskas, R. Ragalevicius, A. Jagminas, R. Tomašiunas, *Optical Investigation and Application of Copper Selenide Nanowires, Lith. J. Phys.* **47** (2007) 361 [doi.org/10.3952/physics.v50i2.1979].

[27] A. Astam, Y. Akaltun, M. Yıldırım, *Conversion of SILAR deposited Cu_3Se_2 thin films to $Cu_{2-x}Se$ by annealing, Mat. Let.* **166** (2016) 9 [doi.org/10.1016/j.matlet.2015.12.030].

[28] M. Li, S. Md Kazi Nazrul Islam, S. Dou, X. Wang, *Significantly enhanced figure-of-merit in graphene nanoplate incorporated Cu2Se fabricated by spark plasma sintering, J. Alloys Compd.* **769** (2018) 59 [doi.org/10.1016/j.jallcom.2018.07.353].

[29] T.P. Bailey, S. Hui, H. Xie, A. Olvera, P. F. P. Poudeu, X. Tang, C. Uher, *Enhanced ZT and attempts to chemically stabilize Cu_2Se via Sn doping, J. Mater. Chem. A* **4** (2016) 17225 [doi.org/10.1039/C6TA06445K].

[30] M. Kieliszek, *Chapter Eleven – Selenium, Adv. Food Nutr. Res.* **96** (2021) 417 [doi.org/10.3390/molecules27196613].

[31] D. Rajesh, R. Rajesh Chandrakanth, C. S. Sunandana, *Annealing Effects on the Properties of Copper Selenide Thin Films for Thermoelectric Applications, IOSR J. Appl. Phys.* **4** (2013) 65 [doi.org/10.9790/4861-0456571].

[32] R. A. M. Napitupulu, *Influence of heating rate and temperature on austenite grain size during reheating steel, IOP Conf. Ser.: Mater. Sci. Eng* **237** (2017) [doi.org/10.1088/1757-899X/237/1/012038].